Impact of Porous Transport Layer Compression on Hydrogen Permeation in PEM Water Electrolysis

Markus Stähler,[a,*] Andrea Stähler,[a] Fabian Scheepers,[a] Marcelo Carmo,[a] Werner Lehnert[a,b] and Detlef Stolten[a,b]

[a]Forschungszentrum Juelich GmbH, Institute of Energy and Climate Research,

IEK-3: Electrochemical Process Engineering, 52425 Juelich, Germany

[b]RWTH Aachen University, Germany

*Corresponding author, tel.: +49 2461 61 2775; fax: +49 2461 61 6695;

E-mail address: m.staehler@fz-juelich.de

Abstract

Gas permeation through a membrane electrode assembly (MEA) is an important issue in the development of polymer electrolyte membrane (PEM) water electrolyzers, because it can cause explosions and efficiency losses. The influence of operating pressure, temperature and MEA modifications on the permeation was already investigated. However, most of the studies pay no attention to the compression of the porous transport layer (PTL) of the MEA when assembling it in a test cell to carry out the experiments.

This paper deals with the impact of the PTL compression on hydrogen permeation and cell voltage. Polarization, impedance and permeation measurements are used to demonstrate that the compression significantly affects the MEA's properties. Measurements show either a linear or nonlinear correlation between current density and hydrogen permeation, depending on the compression.

The results indicate that the compression of the PTL must be taken into account for developing MEAs and comparing different permeation measurements.

Keywords:

PEM water electrolysis, hydrogen permeation, hydrogen crossover, PTL compression, GDL compression

1 Introduction

Gas permeation through a polymer electrolyte membrane (PEM) is still one of the critical gaps in the development of PEM water electrolyzers as the enrichment of hydrogen in oxygen or oxygen in hydrogen can cause a gas explosion [1, 2]. Beyond this safety aspect the permeated gases also reduce the Faradaic efficiency.

Several studies have investigated the hydrogen permeation through a membrane electrode assembly (MEA) for PEM water electrolysis depending on operating conditions and MEA material parameters. Some research groups have studied the influence of gas pressure, temperature and current density on gas permeation and efficiency [3-11]. Others investigated the effect of electrode composition, additional interlayer or membrane modification on MEA performance and gas crossover [12-15]. Most of these studies were performed with MEAs assembled between two porous transport layers (PTL), of which at least one was made of porous carbon material. Trinke et al. demonstrated that increasing the ionomer content in the cathode of a PEM water electrolyzer leads to an increase in the hydrogen permeation and the cell voltage [12]. They explained these increases with a stronger mass transport resistance in the cathode, generated by the higher ionomer content.

Mass transport limitations in an MEA can also be caused by increasing the compression of a carbon PTL, demonstrated for PEM fuel cells in a number of different studies [16]. Mason et al. have shown by means of an impedance study that increasing the compression of the PTL in a PEM fuel cell MEA leads to an increase of the low frequency resistance [17]. This corresponds to the results from Trinke et al. for PEM water electrolysis that a higher ionomer content in the cathode increases the low frequency resistance in the impedance spectra, which corresponds to a higher mass transport resistance [12].

The results of these works suggest that the compression of the PTL in PEM water electrolysis can also affect the mass transport resistance and thus the gas permeation through the membrane. Such a correlation would be of great importance for the further development of PEM water electrolyzers and the comparability of previous studies, as most do not provide any information about the compression of the PTLs used in the experiments.

Thus far, the authors are not aware of any scientific publication in which the dependency between cell compression and hydrogen permeation was examined and that has demonstrated whether this correlation is relevant for the development or not.

For this reason, this work examines the impact of the compression of the carbon PTL on hydrogen permeation and cell performance in PEM water electrolysis by characterizing identical manufactured MEAs with different compression values.

2 Materials and Methods

2.1 MEA preparation

The MEAs used for the described experiments were manufactured by means of the slot die coating and decal method. Anodes and cathodes were first produced by coating iridium dispersion and platinum dispersion respectively on a large sheet of PTFE via slot die, described in detail in Stähler et al. [18]. After drying, coated pieces with dimensions of 4.2 cm x 4.2 cm were cut out. The MEAs were assembled by hot pressing one anode-coated PTFE and one cathode-coated PTFE with a Nafion 212 membrane (thickness: 50 µm) at 130 °C and 0.5 kN/cm² for 3 minutes. The Ir loading at the anode was (0.9 ± 0.03) mg/cm² and the Pt loading at the cathode was (0.25 ± 0.03) mg/cm². The loadings were determined by weighing the coated PTFE pieces before and after the transfer process using an analytical balance (ENTRIS 2241-I, Sartorius, d = 0.1 mg).

2.2 Test cell assembling

The MEAs were combined with porous transport layers for the anode (Ti-felt, Bekipor, Bekaert, thickness 350 +/- 2 µm, coated with iridium on both sides to prevent corrosion [19]) and the cathode side (carbon nonwoven, H23 I2, Freudenberg, thickness 200+/-3 µm). The compression K of the MEA/PTL sandwiches was adjusted by assembling them together with different flat gaskets, as depicted in Figure 1.

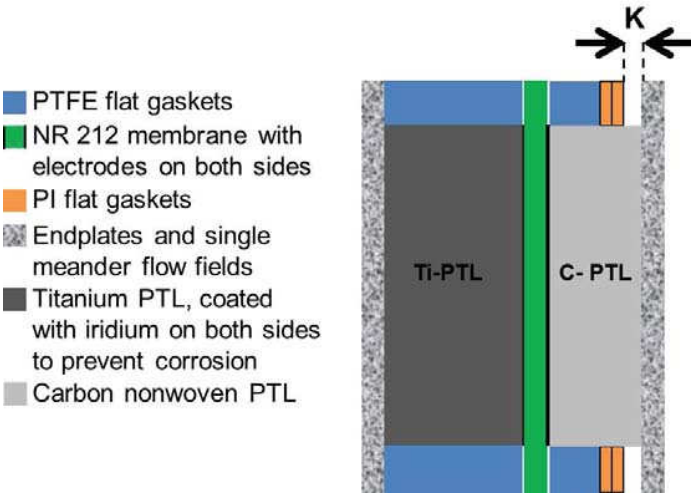

Figure 1. Scheme of the test cell used for the experiments. The compression K of the C-PTL, which is the most flexible material in the layer system, is determined by the thickness of the flat gaskets on the C-PTL-side (PTFE - Polytetrafluorethylen, PI – Polyimid) . The area dimensions are: end plates: (90 x 90) mm², PTLs: (42 x 42) mm². Thicknesses: End plates: 10 mm, Ti-PTL: 0.35 mm, catalyst layer anode side: 0.005 mm, membrane: 0.05 mm, catalyst layer cathode side: 0.003 mm, C-PTL: 0.2 mm.

After mounting the end plates and single meander flow fields (platinized on the anode side, gilded on the cathode side to prevent corrosion), the cell was assembled using nine tie rods. The torque T of the tie rods was increased until the high frequency resistance of the cell, measured with an impedance analyzer (IM6, Zahner) at phase zero, was constant (T = 4 Nm). In this situation, the frame of the flow field is pressed onto the gaskets and the compression of the C-PTL cannot be further increased. The difference between the thickness of the relaxed C-PTL and of the cathode gaskets defines the compression value K for this work.

Preliminary tests with pressure measuring films (Prescale – Fujifilm) in the test cell with a compression value of 100 µm have shown a maximum contact pressure of less than 5 MPa. The compression of the Ti-PTL, which consists of sintered titanium fibers, and the gaskets can be considered negligible for the presented results under these conditions.

2.3 Sample preparation

For the experiments, three MEA samples with different compression values K, presented in Table 1, were assembled in a test cell in accordance with Figure 1. A further MEA (sample 4.X) was first assembled in a test cell with a compression value of K = 25 µm (sample 4.1). After the characterization process, the compression value was increased by about 25 µm by disassembling the cell, removing a 25 µm-thick PI gasket and reassembling the cell (sample 4.2). Then, the characterization measurements were repeated. In a last step, the compression

was further increased by about 25 µm by again removing one 25 µm-thick PI gasket and the measurements were repeated (sample 4.3)

Sample	Compression value K / µm
1	25
2	50
3	90
4.1	25
4.2	50
4.3	75

Table 1. MEA samples with different compression values (thickness of the C-PTL = (200 ± 3) µm) prepared for the experiments.

The comparison of three MEAs with different compression values that are characterized once and one MEA with different compression values characterized three times was chosen to ensure that a measured correlation is due to the compression and not caused by different properties of the different C-PTLs or MEAs used for the experiments.

2.4 Characterization test rig

Figure 2 shows a sketch of the test rig used for the characterization measurements. Deionized water is preheated and pumped into the anode and cathode via peristaltic pumps. Inlet temperatures (T_{ai}, T_{ci}) and outlet temperatures (T_{ao}, T_{co}) of the test cell are monitored to ensure that all temperatures during the experiments are in the temperature range of (80 ± 2)°C. After exiting the temperature-controlled cell, the water/gas mixture is separated by a gas separator on both sides and the water flows back to the reservoirs. While the hydrogen on the cathode side is removed by the exhaust system, the humid oxygen/hydrogen mixture on the anode side is dried by a condenser that cools down the gas up to a dew point of 0.5 °C. The hydrogen content in the oxygen is then measured using a thermal conductivity sensor (FTC300, Messkonzept GmbH).

For impedance measurements, voltages are applied to the cell by an electrochemical workstation (IM6 electrochemical workstation, PP240 power potentiostat, Zahner), whereas a power supply (TDK Lambda, Gen8-600) was used for the polarization measurements.

When measuring the hydrogen concentration in the oxygen flow on the anode side for small current densities, the hydrogen concentration can quickly exceed the safety-relevant value (half of the lower explosion level of 4 vol.% hydrogen in oxygen), at which point the test rig must be

shut down for safety reasons. Additionally, the waiting time to achieve a stable signal when generating only small oxygen flow rates depends strongly on the dead volume of the test rig.

To reduce these disadvantages, the test rig was equipped with two injection points where additional oxygen could be applied to lower the hydrogen concentration (inflow of a diluting oxygen flow $V'_d(O_2)$, see Figure 2) and to reduce the waiting time (inflow of a small flush oxygen flow $V'_f(O_2)$, see Figure 2). By applying a flush flow of 0.04 l/min (flow rates are related to standard conditions: T_s = 273.15 K, p_s = 101325 Pa), the hydrogen concentration signal is stationary within 10 minutes after a current step, even if the current density is in the range of 10 mA/cm². Test measurements have shown that the flush stream has no measurable influence on the cell voltage or current.

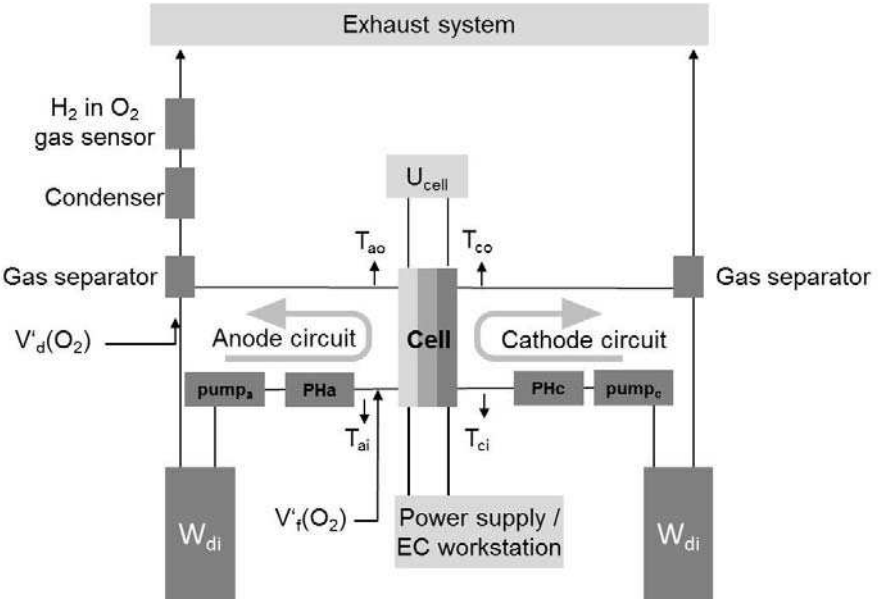

Figure 2. Scheme of the test rig used for the characterization measurements. The temperature-controlled test cell is supplied with preheated deionized water at both sides (PHa, PHc). In this way, temperature gradients in the cell during operation can be reduced. An oxygen flow $V'_f(O_2)$ can also be applied to the anode inlet to flush the cell and reduce the waiting time until the hydrogen sensor signal is stable while an oxygen dilution flow $V'_d(O_2)$ can be used to lower the hydrogen concentration after the cell for safety reasons.

The hydrogen volume fraction ϕ related to the electrochemical produced oxygen can be calculated as follows:

Assuming that hydrogen and oxygen gases behave ideally and the oxygen permeation through the MEA can be neglected, the electrochemical generated oxygen flow rate can be calculated by using the ideal gas law in combination with Faraday's law:

$$V'_{ec}(O_2) = \frac{T_s R}{4F p_s} I = c\, I; \quad c = \frac{T_s R}{4\, F\, p_s} \tag{1}$$

Where I is the total current, T_s and p_s are the standard temperature (273.15 K) and standard pressure (101325 Pa), R is the general gas constant and F is the Faraday constant.

The hydrogen volume fraction, measured by the sensor, is defined by equation (2) and the hydrogen volume fraction related to the electrochemical generated oxygen is defined by equation (3)

$$\phi_{sensor} = \frac{V'(H_{2,perm})}{V'(H_{2,perm}) + V'_f(O_2) + V'_d(O_2) + V'_{ec}(O_2)} \tag{2}$$

$$\phi = \frac{V'(H_{2,perm})}{V'(H_{2,perm}) + V'_{ec}(O_2)} \tag{3}$$

After transforming equation (2) and inserting in equation (3), it follows equation (4) which allows calculating the hydrogen volume fraction Φ related to the electrochemical generated oxygen.

$$\phi = \frac{V'_f(O_2) + V'_d(O_2) + I\, c}{V'_f(O_2) + V'_d(O_2) + \frac{I\, c}{\phi_{sensor}}} \tag{4}$$

The FTC 300 sensor was calibrated by using calibration gases (Linde) with an uncertainty of 2% of the adjusted concentration. For calibrating the FTC 300 sensor, the calibration gases were injected before the anode inlet (see Figure 2, $V'_f(O_2)$ injection point), while the cell was heated to an operating temperature of 80 °C. In this way, the calibration gas was humidified, while the dew point of the gas behind the condenser is identical to the dew point when the cell was driven in characterization mode (T_d = 0.5 °C). The constant dew point for all relevant oxygen dilution and flush flows was checked before the experiments with a dew point mirror (HX 373, MBW) that was temporarily mounted behind the FTC 300 sensor (see Figure 2, behind the H_2 in O_2 gas sensor).

2.5 Characterization Process

After assembling an MEA sample into the test cell and mounting it in the test rig, the pumps began to flush both sides of the cell with deionized water with a flow rate of 0.035 l/min. Then, the preheaters and cell were heated up to 80 °C. One hour later, the characterization measurements began with an impedance measurement at 1.45 V to determine the high frequency resistance. The measurements were followed by a polarization measurement wherein the test cell was driven at different potentials, each for 15 minutes. The potential was increased

from 1.45 V to 1.85 V in 0.05 V steps and then decreased from 1.85 V to 1.45 V in 0.1 V steps to check hysteresis. These voltage values have been chosen to cover the range of 1.0 A/cm² to 3.0 A/cm² relevant for PEM water electrolysis [20]. Lower current density values are of less importance for hydrogen production because of low production rates. But some measurement points in the low current density range were additionally chosen to observe the increase of hydrogen volume fraction at the anode side. The higher voltage limit of 1.75 V was chosen because of the long term target for PEM water electrolyzer system efficiency of approximately 70 % related to lower heating value [20]. As a result, the cell efficiency ($\eta = U_{LHV}/U_{cell}$, $U_{LHV} \approx 1.25$ V) has to be higher than 70 % which means that the cell voltage should be less than about 1.75 V.

The oxygen dilution flow $V'_d(O_2)$ was constant at 0.06 l/min, whereas the oxygen flush flow $V'_f(O_2)$ was set to 0.04 l/min for current densities smaller than 1 A/cm². For larger current densities, the flush stream was turned off.

After the polarization measurement, the impedance measurement was repeated to check whether the high frequency resistance has changed. In case of a change compared to the first measurement, the data from the last measurement were used for evaluation. The high frequency resistance values were used to calculate the iR-free polarization curve, while the hydrogen volume fraction values ϕ were used to calculate the permeation current density i_P, defined by equation (5):

$$i_P = \frac{\phi}{1-\phi}\,\frac{i}{2} \tag{5}$$

Where i is the electric current density, the volume fraction ϕ is calculated according to equation (4).

3 Results and discussion

The measured polarization and concentration data of samples 1-3, which were each characterized with a specified compression, are shown in Figure 3 A. The results of the samples 4.X, which was characterized three times, each time with a higher compression, are presented in Figure 3 B.

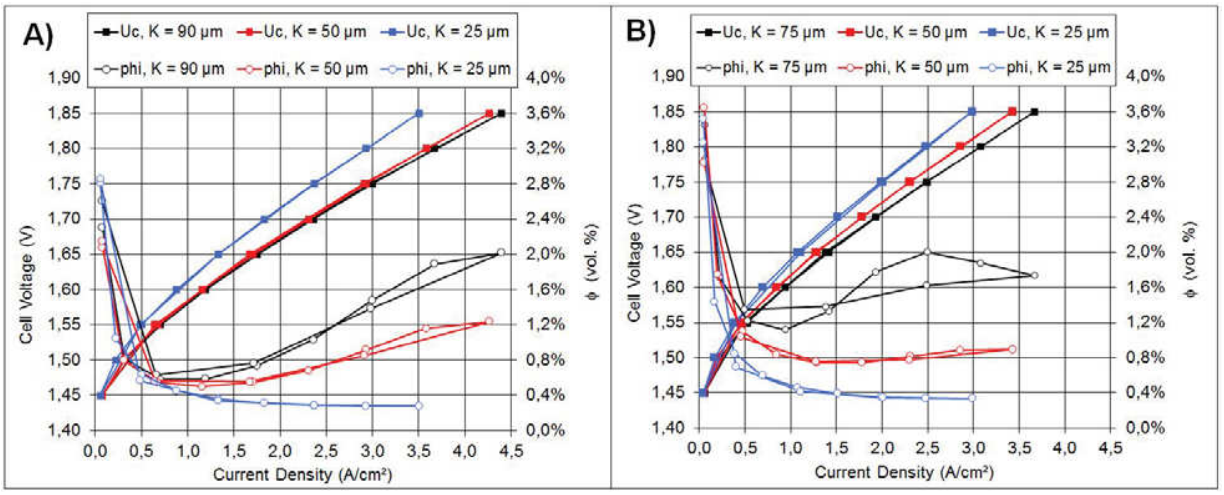

Figure 3. Cell voltages (filled squares) and hydrogen volume fraction ϕ (open circles), calculated according to equation (4), as a function of current density i. A) Data of samples 1-3 with different compression values K characterized once; B) data of sample 4 characterized three times, each time with an increased compression value K.

Both diagrams show, the higher the compression value K is, the lower the cell voltages. Furthermore, the hydrogen volume fraction increases significantly for higher compression values and higher current densities. For low current densities when only less oxygen is produced, a small amount of hydrogen permeates from cathode to anode. This amount of hydrogen depends on membrane thickness and partial pressure but not on current density [3]. As a result, the less oxygen is produced or the smaller the current density, the higher the hydrogen concentration in the oxygen.

It can be noted that the MEAs that were investigated in this study show a hysteresis in the hydrogen volume fraction curve that was more pronounced the stronger the compression was. However, the cause of this hysteresis could not be clarified in this study.

While the hydrogen volume fraction in Figure 3 A and Figure 3 B are very similar for a compression value K = 25 µm, there are clearly visible differences between the curves for higher compression values. At this point it has to be taken into account that sample 4.X was assembled

and disassembled several times to realize different compression values with the same MEA. The impact of this procedure on the polarization values and especially the hydrogen permeation is unknown. The reason for characterizing sample 4.1, 4.2 and 4.3 was to ensure that the measured correlation for sample 1, 2 and 3 is due to the compression and not caused by different properties of the different C-PTLs or MEAs used for the experiments. The same trend in the hydrogen permeation curves in Figure 3 B when increasing the compression values confirms therefore the trend in Figure 3 A between the compression of the C-PTL and the hydrogen permeation curve.

The reason for the correlation between the compression and cell voltage in PEM fuel cells has already been described in different studies [17, 21]. Thus, the higher compression of the carbon PTLs reduces the porosity and increases the contact pressure on the electrode, which lowers the Ohmic voltage losses. This results in lower cell voltages in PEM water electrolysis and higher cell voltages in PEM fuel cells. The lower electrical resistances for higher compression values K can be confirmed in this work by smaller high frequency resistances (R) in the measured impedance data, which are presented in Table 2.

Sample	Compression value K in µm	High frequency resistance R in Ωcm²
1	25	0.085 ± 0.002
2	50	0.064 ± 0.002
3	90	0.058 ± 0.002
4.1	25	0.099 ± 0.002
4.2	50	0.083 ± 0.002
4.3	75	0.070 ± 0.002

Table 2. High frequency resistance values R of the samples, extracted from the impedance data. The uncertainties are estimated on the base of the accuracy in the determination from impedance spectra measurements. The uncertainty values in the table represents the single standard deviation.

The different resistance values R in Table 2 for same compression value K but different samples are (0,014±0.003) Ωcm² (difference between $R_{\text{sample 4.1, K= 25 µm}}$ and $R_{\text{sample 1, K=25 µm}}$) respectively (0,019±0.003) Ωcm² (difference between $R_{\text{sample 4.2, K=50 µm}}$ and $R_{\text{sample 2, K= 50 µm}}$). These differences are comparable within the measurement uncertainty and are assigned to the different Ti-PTLs used for the experiments. One Ti-PTL was used for sample 1, 2 and 3 and another one for sample 4.1, 4.2 and 4.3. Because of this difference, the disagreement of the polarization curves in Figure 3 A and B for the samples with a compression value of 25 µm can be fully explained within the uncertainty of the experiment by the different Ti-PTLs used for the measurements.

Because of the above explanation regarding the compression and the resistance, it is very likely that the higher the C-PTL is compressed the more hydrogen is retained in the cathode. This is synonymous with an increased mass transport resistance for the hydrogen from the cathode to flow field. This mass transport resistance results in stronger hydrogen permeation through the membrane the more hydrogen is produced at the cathode (see Figure 3 A and B, with increasing of the hydrogen volume fraction for current density values larger than 1 to 1.5 A/cm²).

According to Trinke et al., an increase in the ionomer content in the cathode leads to an increase in mass transport resistance for the hydrogen. This increases the hydrogen concentration at the cathode and thus the hydrogen permeation through the membrane [12]. Furthermore, they have shown that according to the Nernst equation, the higher hydrogen concentration can result in smaller cathodic half-cell potentials and thus in higher cell voltages.

If one transfers this argumentation to the data presented in Figure 3, the increase in the hydrogen permeation for higher current densities could be interpreted as an increase in the hydrogen concentration at the cathode. As a consequence, this should result in higher cathodic half-cell potentials and therefore in an increase in the cell voltage. In particular, the increase in the volume fraction data in Figure 3 for current densities larger than 1 to 1.5 A/cm² should be correlated with a significant increase in the iR-free cell voltages.

To determine if this correlation exists in the measured data, the data are recalculated: the polarization values from Figure 3 are used in combination with the high frequency resistance values from Table 2 to calculate the iR-free cell voltages by subtracting the Ohmic part ($i \cdot R$) from the measured cell voltages. Additionally, the hydrogen volume fraction data from Figure 3 are transformed into the permeation current density according to equation (5) to get a hydrogen flow-specific unit.

The results, presented in Figure 4, show a change in the order of the polarization curves in comparison to Figure 3. The iR-free cell voltages for the stronger compressed MEA samples are slightly smaller for current densities smaller than 1 A/cm². But the voltage values increase more strongly for larger current densities when the compression value is higher. Hence, the slope in the iR-free cell voltage curves is higher. This fits very well with the observation from Trinke et al., that higher ionomer content in the cathode induces a higher mass transport resistance, which leads to a higher slope of the polarization curve [12].

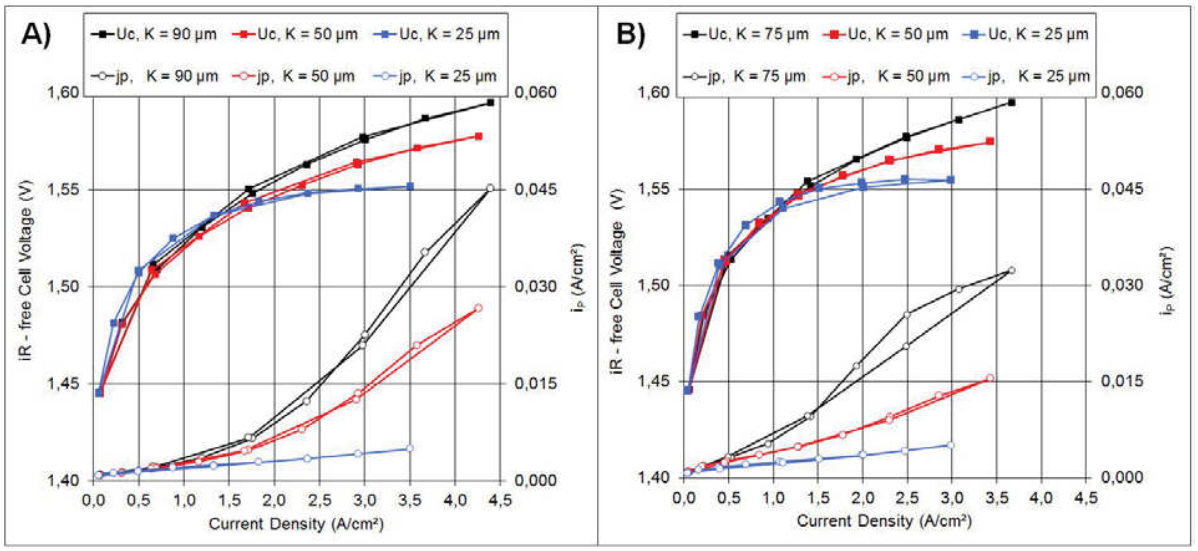

Figure 4. iR-free cell voltages (filled squares) and permeation current densities i_p (open circles) as a function of current density i. A) Data of samples 1-3 with different compression values K characterized once; B) data of sample 4 characterized three times, each time with an increased compression value K.

The direct comparison of the polarization and hydrogen volume fraction curves in Figure 4 A and Figure 4 B shows differences, but regarding the above reasoning the comparison should only be made for samples with compression value of 25 µm. For K = 25 µm, the difference in the polarization date of Figure 4 A and Figure 4 B are smaller than 10 mV which is still in the range of uncertainty. According to the data in Table 2, the reason for the smaller current densities in the curves of Figure 4 B is the larger high frequency resistance of the Ti-PTL used for sample 4.X.

These results show that the compression of the C-PTL in a PEM water electrolyzer cell not only influences the hydrogen permeation and cell voltage. In contrast to other studies, which applied current densities of up to 2 A/cm² at maximum when measuring the hydrogen permeation, the data in Figure 4 additionally demonstrates that the strength of the C-PTL compression also affects the type of correlation between i_p and i: whether it is linear or not depends on the compression in the C-PTL, clearly visible in the current density range of up to 4 A/cm² in Figure 4.

4 Conclusions

This study demonstrates a correlation between the hydrogen permeation through a membrane of an MEA for PEM water electrolysis and the compression of the carbon porous transport layer under ambient pressure. Furthermore, it is shown that the correlation between electric current density and permeation current density can be nonlinear, depending on the compression used.

These results are important for comparing data from different experiments that use different MEA compressions. Without specifying the compression, the results can hardly be compared. The results are also meaningful for the development of test cells and stacks for PEM water electrolysis, as they show how sensitively the hydrogen permeation can react on compression differences and therefore how precise cell and stack components must be produced.

Up until now, the findings can be described but currently the question as to why the hydrogen permeation depends so strongly on a compression difference within the MEA cannot be explained by the authors. Further research work is necessary to understand the physical and electrochemical processes within the MEA to find concepts to reduce the hydrogen permeation in MEAs for PEM water electrolysis.

Acknowledgements

We convey our thanks to Thomas Pütz for his indispensable support of this work.

References:

[1] Babic U, Suermann M, Buehi FN, Gubler L, Schmidt TJ. Review-Identifying Critical Gaps for Polymer Electrolyte Water Electrolysis Development. Journal of the Electrochemical Society. 2017;164:F387-F99.
[2] Grigoriev SA, Millet P, Korobtsev SV, Porembskiy VI, Pepic M, Etievant C, et al. Hydrogen safety aspects related to high-pressure polymer electrolyte membrane water electrolysis. Int J Hydrog Energy. 2009;34:5986-91.
[3] Schalenbach M, Carmo M, Fritz DL, Mergel J, Stolten D. Pressurized PEM water electrolysis: Efficiency and gas crossover. Int J Hydrog Energy. 2013;38:14921-33.
[4] Schalenbach M. Corrigendum to "Pressurized PEM water electrolysis: Efficiency and gas crossover" [Int J Hydrogen Energy 38 (2013) 14921–14933]. Int J Hydrog Energy. 2016;41:729-32.
[5] Trinke P, Bensmann B, Reichstein S, Hanke-Rauschenbach R, Sundmacher K. Hydrogen Permeation in PEM Electrolyzer Cells Operated at Asymmetric Pressure Conditions. Journal of the Electrochemical Society. 2016;163:F3164-F70.
[6] Trinke P, Bensmann B, Reichstein S, Hanke-Rauschenbach R, Sundmacher K. Impact of Pressure and Temperature on Hydrogen Permeation in PEM Water Electrolyzers Operated at Asymmetric Pressure Conditions. In: Jones DJ, Uchida H, Gasteiger HA, SwiderLyons K, Buchi FN, Pintauro P, et al., editors. Polymer Electrolyte Fuel Cells 16. Pennington: Electrochemical Soc Inc; 2016. p. 1081-94.
[7] Trinke P, Bensmann B, Hanke-Rauschenbach R. Experimental evidence of increasing oxygen crossover with increasing current density during PEM water electrolysis. Electrochemistry Communications. 2017;82:98-102.
[8] Trinke P, Bensmann B, Hanke-Rauschenbach R. Current density effect on hydrogen permeation in PEM water electrolyzers. Int J Hydrog Energy. 2017;42:14355-66.
[9] Trinke P, Haug P, Brauns J, Bensmann B, Hanke-Rauschenbach R, Turek T. Hydrogen Crossover in PEM and Alkaline Water Electrolysis: Mechanisms, Direct Comparison and Mitigation Strategies. Journal of the Electrochemical Society. 2018;165:F502-F13.
[10] Ito H, Miyazaki N, Ishida M, Nakano A. Cross-permeation and consumption of hydrogen during proton exchange membrane electrolysis. Int J Hydrog Energy. 2016;41:20439-46.
[11] Bessarabov D, Kruger AJ, Luopa SM, Park J, Molnar AA, Lewinski KA. Gas Crossover Mitigation in PEM Water Electrolysis: Hydrogen Cross-over Benchmark Study of 3M's Ir-NSTF Based Electrolysis Catalyst-Coated Membranes. In: Jones DJ, Uchida H, Gasteiger HA, SwiderLyons K, Buchi FN, Pintauro P, et al., editors. Polymer Electrolyte Fuel Cells 16. Pennington: Electrochemical Soc Inc; 2016. p. 1165-73.
[12] Trinke P, Keeley GP, Carmo M, Bensmann B, Hanke-Rauschenbach R. Elucidating the Effect of Mass Transport Resistances on Hydrogen Crossover and Cell Performance in PEM Water Electrolyzers by Varying the Cathode Ionomer Content. Journal of the Electrochemical Society. 2019;166:F465-F71.
[13] Bernt M, Gasteiger HA. Influence of Ionomer Content in IrO2/TiO2 Electrodes on PEM Water Electrolyzer Performance. Journal of The Electrochemical Society. 2016;163:F3179-F89.
[14] Klose C, Trinke P, Bohm T, Bensmann B, Vierrath S, Hanke-Rauschenbach R, et al. Membrane Interlayer with Pt Recombination Particles for Reduction of the Anodic Hydrogen Content in PEM Water Electrolysis. Journal of the Electrochemical Society. 2018;165:F1271-F7.
[15] Garbe S, Babic U, Nilsson E, Schmidt TJ, Gubler L. Communication—Pt-Doped Thin Membranes for Gas Crossover Suppression in Polymer Electrolyte Water Electrolysis. Journal of The Electrochemical Society. 2019;166:F873-F5.
[16] Khetabi E, Bouziane K, Zamel N, Francois X, Meyer Y, Candusso D. Effects of mechanical compression on the performance of polymer electrolyte fuel cells and analysis through in-situ characterisation techniques - A review. Journal of Power Sources. 2019;424:8-26.
[17] Mason TJ, Millichamp J, Shearing PR, Brett DJL. A study of the effect of compression on the performance of polymer electrolyte fuel cells using electrochemical impedance spectroscopy and dimensional change analysis. Int J Hydrog Energy. 2013;38:7414-22.

[18] Stähler M, Stähler A, Scheepers F, Carmo M, Stolten D. A completely slot die coated membrane electrode assembly. Int J Hydrog Energy. 2019;44:7053-8.
[19] Liu C, Carmo M, Bender G, Everwand A, Lickert T, Young JL, et al. Performance enhancement of PEM electrolyzers through iridium-coated titanium porous transport layers. Electrochemistry Communications. 2018;97:96-9.
[20] Bertuccioli L, Chan A, Hart D, Lehner F, Madden B, Standen E. Development of Water Electrolysis in the European Union. Fuel Cells HydrogenJoint Undertakings, Lausanne 2014.
[21] Qiu D, Janßen H, Peng L, Irmscher P, Lai X, Lehnert W. Electrical resistance and microstructure of typical gas diffusion layers for proton exchange membrane fuel cell under compression. Applied Energy. 2018;231:127-37.